

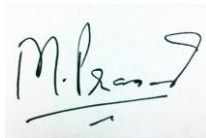
DOE Award No.: DE-FE-0009963

Quarterly Research Performance Progress Report (Period ending 12/31/2016)

Measurement and Interpretation of Seismic Velocities and Attenuations in Hydrate-Bearing Sediments

Project Period (10/1/2012 to 12/31/2016)

Submitted by:
co-PI: Manika Prasad
Colorado School of Mines
DUNS #010628170.
1500 Illinois Street
Golden, CO 80401
e-mail: mprasad@mines.edu
Phone number: (303) 273-3457
Submission Date: 1/31/2017



Prepared for:
United States Department of Energy
National Energy Technology Laboratory



Office of Fossil Energy

Disclaimer

This report was prepared as an account of work sponsored by an agency of the United States Government. Neither the United States Government nor any agency thereof, nor any of their employees, makes any warranty, express or implied, or assumes any legal liability or responsibility for the accuracy, completeness, or usefulness of any information, apparatus, product, or process disclosed, or represents that its use would not infringe privately owned rights. Reference herein to any specific commercial product, process, or service by trade name, trademark, manufacturer, or otherwise does not necessarily constitute or imply its endorsement, recommendation, or favoring by the United States Government or any agency thereof. The views and opinions of authors expressed herein do not necessarily state or reflect those of the United States Government or any agency thereof.

Abstract

Measurement and Interpretation of Seismic Velocities and Attenuations in Hydrate-Bearing Sediments

Grant/Cooperative Agreement DE-FE 0009963.

Free water presence: We successfully performed electrical conductivity measurements on Castlegate Sandstone samples before and after methane hydrate formation. Our measurements show that we can distinguish initiation and completion of the hydrate formation process. Our electrical conductivity measurements also corroborated our previously reported observation that even after the hydrate formation was completed, we still had free water in the sample which was turned into ice after lowering the temperature below the freezing point of water.

Hydrate Location: We performed ultrasonic velocity measurements on Ottawa Sand (F110) with different THF hydrate saturations (60% and 40%). We observe increasingly smaller velocity increases due to hydrate formation with decreasing hydrate saturation. This observation suggests that at low concentration, hydrate are not cementing. A further confirmation of non-cementing hydrates at low hydrate concentration is the larger increase in velocities with increasing confining pressure. A cementing hydrate would create a stiffer framework and prevent large compaction-driven increases in velocity. We also find that the effect of hydrate cementation is more pronounced in V_p - V_s ratios. These measurements provide a diagnostic tool to detect hydrate saturations.

Data comparison and dissemination: We obtained velocity and attenuation data for methane hydrates formed using the excess gas and excess water method. Data from the excess gas method shows that already small amounts of hydrate have a strong influence on the v_p - v_s ratio (hydrate saturations of about 3%). Whereas the data from methane hydrates formed with the excess water method shows that changes start to occur at higher gas hydrate saturations (>30 %). A comparison of methane hydrate data formed using the excess water method with our THF hydrate data show a great match. In both cases, the decreases in V_p - V_s ratio with increasing hydrate saturation are comparable.

Measurement system: We built a new set of ultrasonic P-wave transducers and a new aluminum pressure cell for the use inside of the CT scanner with a bigger inner diameter than the previously used Torlon cell. The cell has been pressure tested and the ultrasonic transducers have been proven to work.

Table of Contents

Disclaimer	1
Abstract	3
Table of Contents	4
List of Figures and Tables	5
<i>List of Figures</i>	5
<i>List of Tables</i>	5
2. Accomplishments	6
2.1 <i>Overview of Milestone Status</i>	6
2.2 <i>Resistivity Measurements on Hydrate Bearing Sediments (continued)</i>	10
2.3 <i>Velocity Measurements of THF hydrate bearing Ottawa Sand</i>	13
2.4 <i>Loss Diagram (continued)</i>	15
2.5 <i>Updates to Micro X-Ray CT Pressure Control Setup</i>	17
3. Acknowledgments	20
4. Plans	22
5. Products	23
6. Participants and Collaborating Organizations	24
7. Changes / Problems	27
8. Special Reporting Requirements	28
9. Budgetary Information	29

List of Figures and Tables

List of Figures

Figure 1: Milestone Status. We are at the end of our 17th quarter and in the final phase of this project. In February 2016, we requested and were granted a no-cost extension until December 31, 2016.....	6
Figure 2: Real and imaginary conductivity for all 92 measurements of the experiment for one frequency.....	12
Figure 3: Stage 1 of the experiment - Cooling.....	13
Figure 4: Average ultrasonic velocities for 80% (squares), 60% (circles), and 40% (triangles) THF hydrate bearing samples. Numbers are explained in Table 1.	14
Figure 5: Average Compressional and shear wave velocity ratios for 80% (squares), 60% (circles), and 40% (triangles) THF hydrate bearing samples. Numbers are explained in Table 1.....	15
Figure 6: Loss diagram with data provided from Priest as well as well log data from Guerin & Goldberg.....	16
Figure 7: Loss Diagram with our obtained average vp-vs ratios for 80% (4), 60% (3), and 40% (2) THF hydrate in Ottawa sand and our samples containing THF-water mixture (1). The arrows indicate increase in hydrate saturation.....	17
Figure 8: Aluminum pressure cell for use inside CT scanner.....	18
Figure 9: Ultrasonic P-wave transducers for use inside micro CT scanner.....	18
Figure 10: Waveforms for 4 pieces of aluminum – 19.5 mm, 47.6 mm, 67.5 mm and 102.1 mm long.....	20
Figure 11: arrival times for all 4 aluminum pieces (blue) and dead time (yellow)	20

List of Tables

Table 1: Milestone status	7
Table 2: Clarification for numbers in Figure 4.	14
Table 3: Q17 Milestones and Deliverables.....	22

2. Accomplishments

2.1 Overview of Milestone Status

This report marks the end of our project. Our current position is shown in the time chart in Figure 1 and the Milestone status is shown in

Table 1. Note that we were granted a no-cost extension until December 31, 2016. In the current period of Q15 (Q3 of Year 4), we continued our work on Task 9 – MXCT Characterization and Task 6 – CH₄-hydrate bearing rock (free gas). Figure 2 shows the status and date of completion for each Milestone.

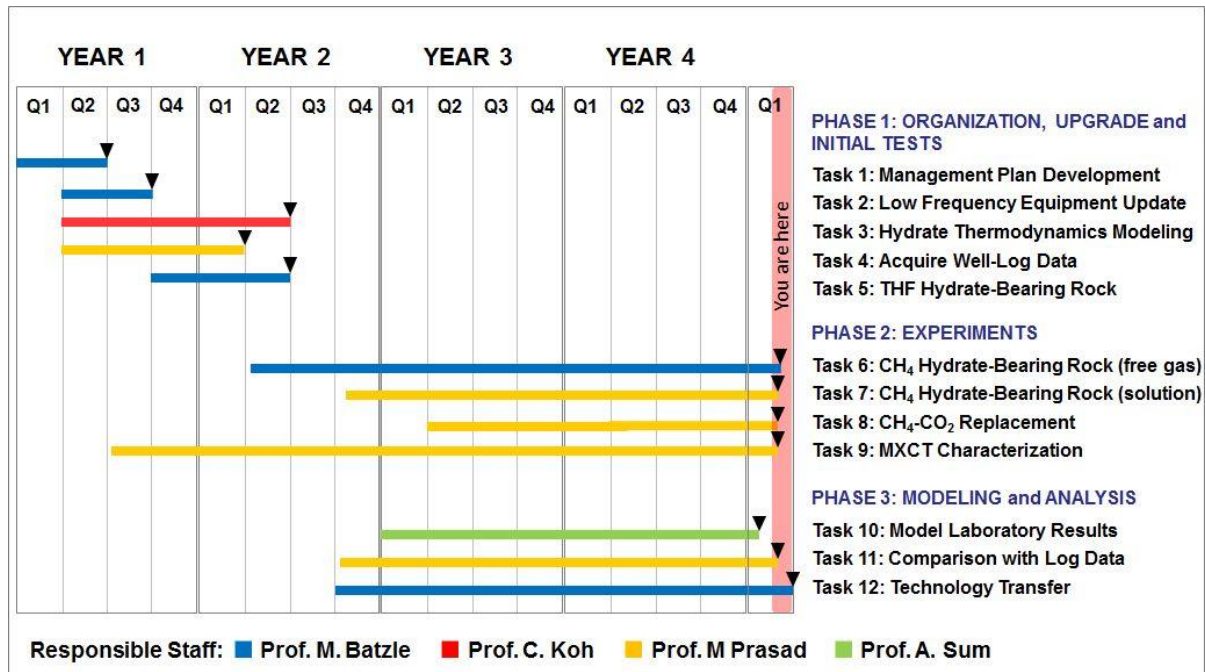


Figure 1: Milestone Status. We are at the end of our 17th quarter and in the final phase of this project. In February 2016, we requested and were granted a no-cost extension until December 31, 2016.

Table 1: Milestone status

Milestone	Title / Description	Status	Date: expected completed or)
Completed			
PHASE 1: ORGANIZATION, UPGRADES, INITIAL TESTS			
Task 1	Project Management Plan Development	Complete & approved	1-Dec-12
Task 2	Low Frequency Equipment Upgrades	Completed	1-Jun-13
Task 3	Hydrate Thermodynamic Modeling	Completed	31-May-14
Task 4	Acquire In Situ Data (logs)	Completed	31-May-14
Task 5	THF hydrate-saturated Rock measurement	Completed	15-Jun-14
Task 6	THF hydrate grown in pressure vessel	Completed	15-Apr-14
Continuing or Planned			
Task 7	CH4 hydrate from free gas Measurements	Continuing*	1-Oct-16
Task 8	CH4 hydrate (gas in solution) measurement	Planned	31-Oct-16
Task 9	CO2-CH4 replacement hydrate measurement	Planned	30-Oct-14
Task 10	MXCT Scanning Characterization	Continuing*	31-Dec-16
Task 11	Model Laboratory Measurements	Continuing*	30-Nov-16
Task 12	Comparison with Log Data	Planned	30-Nov-16
Task 13	Technology Transfer	Continuing*	31-Dec-16
* initial stages were completed on schedule, but the process continues throughout the project			

Milestone	Title / Description	Status towards completion / Date of Completion
Task 1	Project Management Plan Development	Complete & approved Date: 12/1/2012
Task 2	Low Frequency Equipment Upgrades	Complete & approved Date: 6/1/2013
Task 3	Hydrate Thermodynamic Modeling	Complete & approved Date: 5/31/2014
Task 4	Acquire In Situ Data (logs)	Complete & approved Date: 5/31/2014
Task 5	THF hydrate-saturated Rock measurement	Complete & approved Date: 6/15/2014
Task 6	THF hydrate grown in pressure vessel	Complete & approved Date: 4/15/2014
Task 7	CH ₄ hydrate from free gas Measurements	Success: Made hydrates from free gas and have conducted electrical measurements on the CH ₄ hydrate bearing sediments. Completed acoustic measurements. (Students will continue to perform experiments as part of their theses. Date: 1/31/2017
Task 8	CH ₄ hydrate (gas in solution) measurement	Unsuccessful – but not realistic to complete by 12/31: We had planned this work however, the experiments were not successful Date: 12/31/2016.
Task 9	CO ₂ -CH ₄ replacement hydrate measurement:	Abandoned: After reading various other studies and consulting with our co-I, Dr. Carolyn Koh, and given the delays in equipment reliability, we decided to abandon these efforts and focus instead on the CH ₄ hydrates first.
Task 10	MXCT Scanning Characterization	Success: Completed MXCT scans of various hydrates that made in our labs. The in situ hydrate imaging under pressure is also completed Date: 12/31/2016.

Figure 2. Milestone status with dates of completion for each Milestone (continued on next page).

Task 11	Model Laboratory Measurements	<p>Success: Created models to explain experimental data in context of the various hydrate-forming habits. The most rewarding aspect of our work has been that we can demonstrate a gradual shift of hydrates from pore filling to framework and cementing locations with increasing hydrate concentration</p> <p>Date: 1/31/2017.</p>
Task 12	Comparison with Log Data	<p>Success: Here, we have compiled a large amount of data both in our own laboratories as well as from other researchers. This compilation of data shows clearly that we should be able to separate large concentrations of hydrates in sediments from minor amounts using shear and compressional wave data.</p> <p>Date: 10/31/2016.</p>
Task 13	Technology Transfer	<p>Success: Two papers published, numerous conference papers (SEG, ICGH, AGU); one paper accepted; two more papers underway.</p> <p>Date: 10/31/2016.</p>

Figure 2. Milestone status with dates of completion for each Milestone.

2.2 Resistivity Measurements on Hydrate Bearing Sediments (continued)

As already reported in Q15 we started measuring complex resistivity in sandstones before, during and after hydrate formation.

In this quarter we measured one of the Castlegate sandstone samples (CG1). The measured conductivity (real and imaginary part) for one frequency is shown in Figure 2 for the whole length of the experiment.

So far, the experiment can be divided into 4 stages.

Stage 1: Pressurization and Cooling

The prepared sandstone was taken out of the desiccator where it had been exposed to humidity until it reached full saturation. The sample was placed into the pressure vessel and measured for the first time at atmospheric pressure (Figure 3). The second measurement was conducted after applying methane with a pressure of 1500 psi onto the sample. As we can see, the conductivity value between the first and the second measurement does not vary. After the second measurement, the cooling of the sample started. Measurement 3 and 4 only show small changes in conductivity (Figure 4) which is due to the change in temperature. Once within the hydrate stability temperature we observed a drop in conductivity between measurement 4 and 5 which indicated the start of the hydrate formation within the sandstone. We continued measuring at 1 hour intervals for the next 6 hours and observed a further decrease in conductivity due to further hydrate formation.

Stage 2: Stabilization

During this stage we kept the temperature constant (~ 3.5 °C) and continued measuring for about 2 weeks. We saw no changes occurring in the real part of the conductivity values during this period of time indicating that the conversion of water and methane to hydrate must have stopped. However, looking at the imaginary part shows a continuous drop of conductivity over time (Figure 2).

Stage 3: Freezing

To insure complete conversion of water to hydrate, we lowered the temperature to below the freezing point of water (~ -2 °C). As we can see, we have another sharp drop in conductivity once the sample is below 0 °C indicating that in the sample was residual water present. Also, over time the conductivity value is dropping and not reaching a constant value. During this stage we also observed a power outage which lasted for about 2 hours causing the cooling bath to stop working. During these two hours the sample warmed up to about 4 °C which is still within the hydrate stability temperature but above the freezing point of water causing the sample to start thawing. After the power was back the sample was brought back to ~ -2 °C.

Stage 4: Thawing

In this stage the temperature was brought back to about the temperature value we had before Stage 3 causing existing ice to melt. Even though the cooling bath was set to the same temperature we had during stage 2, the temperature inside the vessel did not go above 2°C. Therefore we had to increase the cooling bath temperature step by step to reach a value of about 3.5 °C. With the same temperature conditions, we are now able to compare our measured conductivities from stage 2 with stage 4. As we can see, the real part of the conductivity is about the same value whereas the imaginary part shows a much larger difference.

Interpretation:

Lowering the temperature to below the freezing point of water caused any available water to freeze. This was observed by an additional drop in conductivity. As a result of the formation of ice the hydrate layer was broken off and after thawing the ice back to water, that water formed more hydrate. This additional formation of hydrate can be seen in the imaginary part of the conductivity. To understand this, we have to understand what the real and imaginary part of the conductivity mean. The real part of the measured conductivity can be seen as the bulk property of the rock whereas the imaginary part measures the conductivity along the grain surfaces of the rock. Even though the water contained in humidity is deionized the grains themselves have cations which become part of the water – the water naturally becomes more conductive. During the second hydrate formation in stage 4 the residual water becomes less but charged with more ions therefore the imaginary part of the conductivity is higher than during the 2 stage.

Results:

With the measured conductivity we can distinctively determine when hydrate formation started and when it ended, as well as that not all of the water was converted into hydrate. Additionally, we showed that forming ice underneath the hydrate layer caused it to break up and making more water available for hydrate formation after thawing the ice.

Real & Imaginary Conductivity @ 23.44 Hz

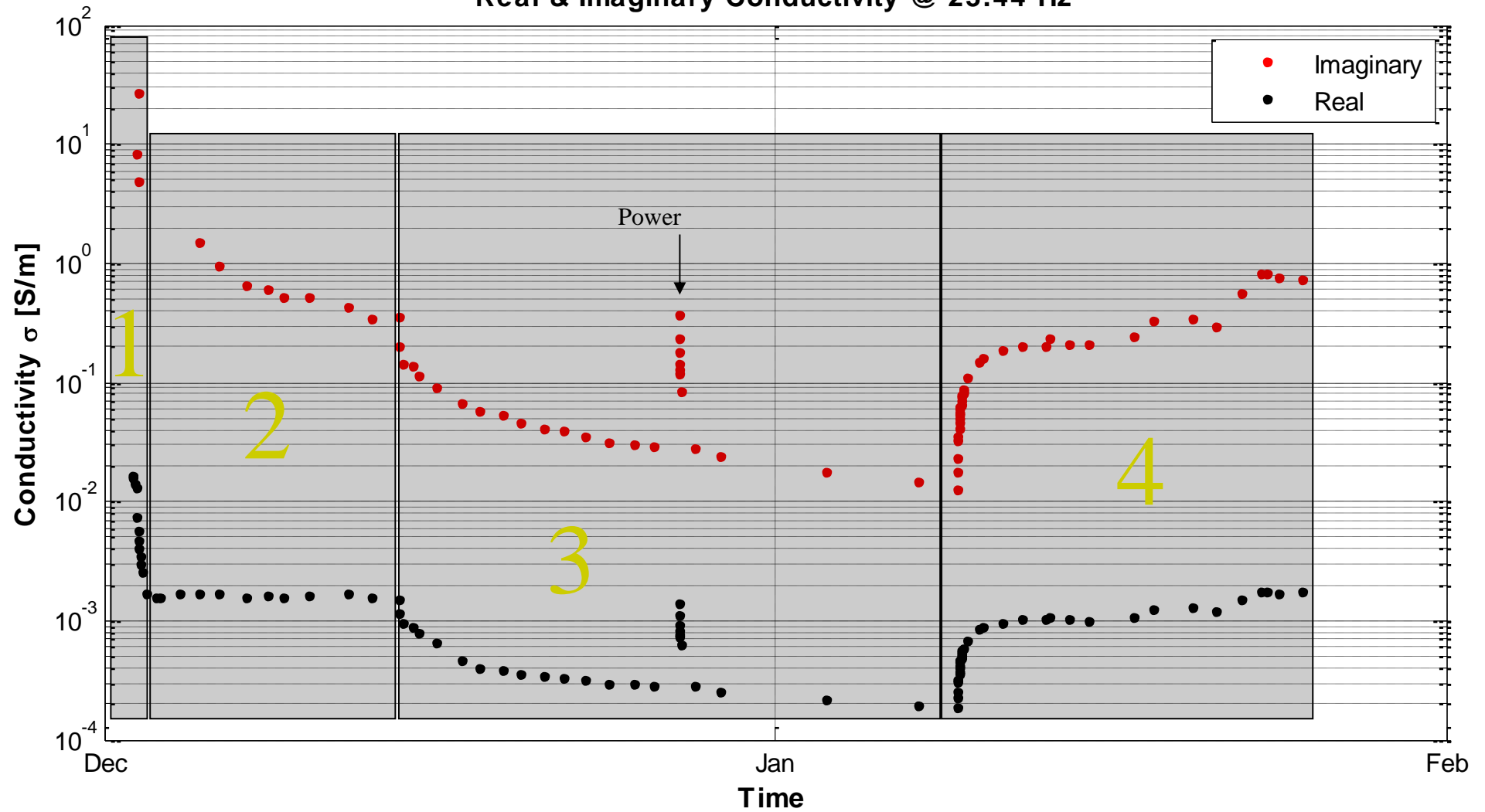


Figure 3: Real and imaginary conductivity for all 92 measurements of the experiment for one frequency

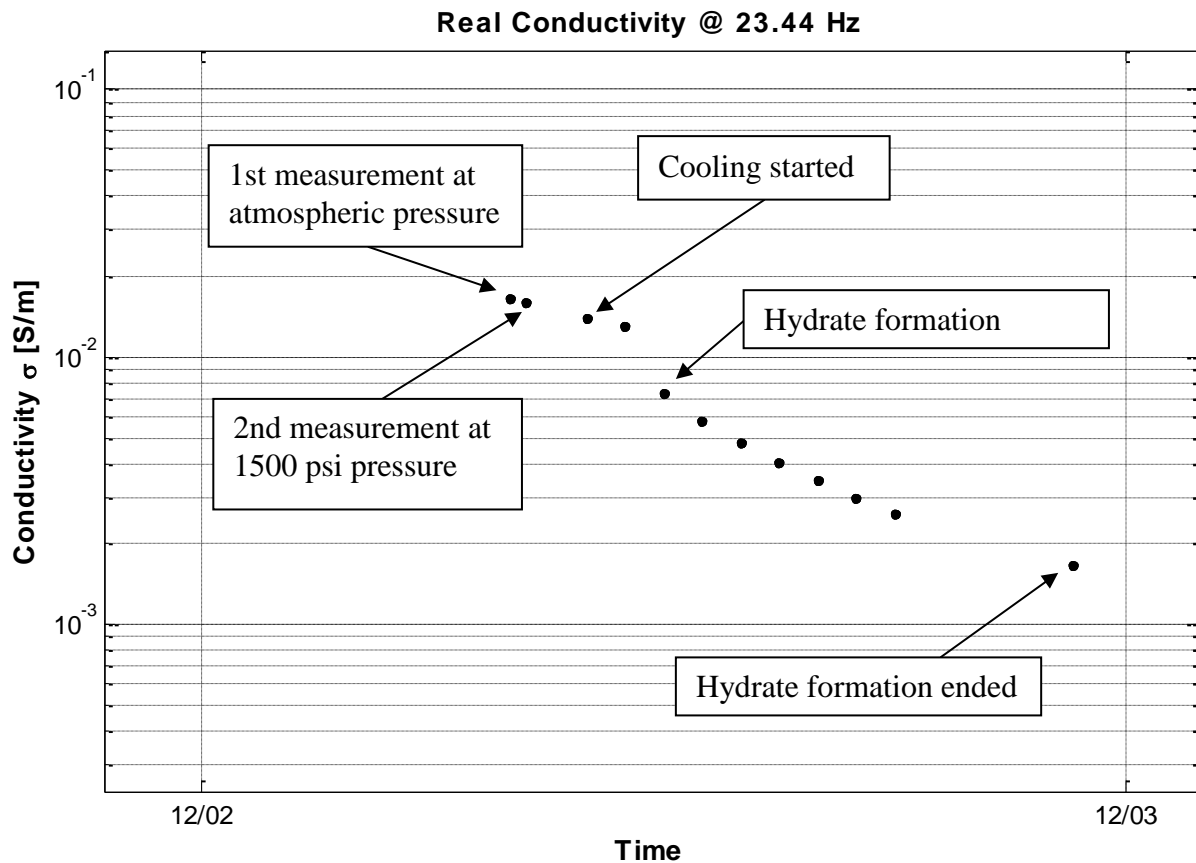


Figure 4: Stage 1 of the experiment - Cooling.

2.3 Velocity Measurements of THF hydrate bearing Ottawa Sand

We continued conducting ultrasonic velocity measurements in Ottawa Sand F110 with 60 % and 40 % THF hydrate.

As we can see in Figure 5, with lower hydrate saturation the measured compressional and shear wave velocities were lower. An additional increase in velocity was observed after an increase in confining pressure to 2275 psi. After hydrate dissociation (stage 5), the velocities dropped to around the starting velocities (stage 1). An additional increase in confining pressure was performed for after hydrate dissociation (only for samples with 60% and 40% THF-water mixture). Both sets of experiments show the same increase in velocity with elevated pressures to 2275 psi.

Figure 6 shows the average compressional and shear wave ratios for all the sets of experiments. As we can see, after hydrate formation (stage 2) the ratios for the velocities decrease. This is due to the cementation caused by the hydrate and which causes a stronger increase in velocity in the shear wave. However, having a closer look we can clearly distinguish the amount of cementation based on hydrate saturation. We can observe the strongest cementation effect in the 80% hydrate saturated sample. For the 60% hydrate sample we can see an increased v_p - v_s ratio and an even higher v_p - v_s ratio for 40% hydrate saturation. This means we observed the weakest cementation effect for samples containing the lowest amount of hydrates. However, after increasing the confining pressure to 2275 psi, we can see a strong decrease in the v_p - v_s ratio for the 40 % and 60 % hydrate saturated samples. The change in ratio for the 80% hydrate with increased confining pressure is only minimal. This means that the sample containing 80% hydrate must be mainly supported by the hydrate matrix whereas the samples containing 40 and 60% hydrate are both, supported by the hydrate as well as grain matrix. After reducing the pressure back to 435 psi, the v_p - v_s ratios return to the values they were before increasing the

pressure. After dissociation, the vp-vs ratios are lower than at the beginning of the experiments. This indicates a cementation process must have occurred to the grain matrix – either due to the formation of hydrate or due to the introduced pressure cycle. After the dissociation and applying a pressure of 2275 psi we can see another drop in the vp-vs ratio.

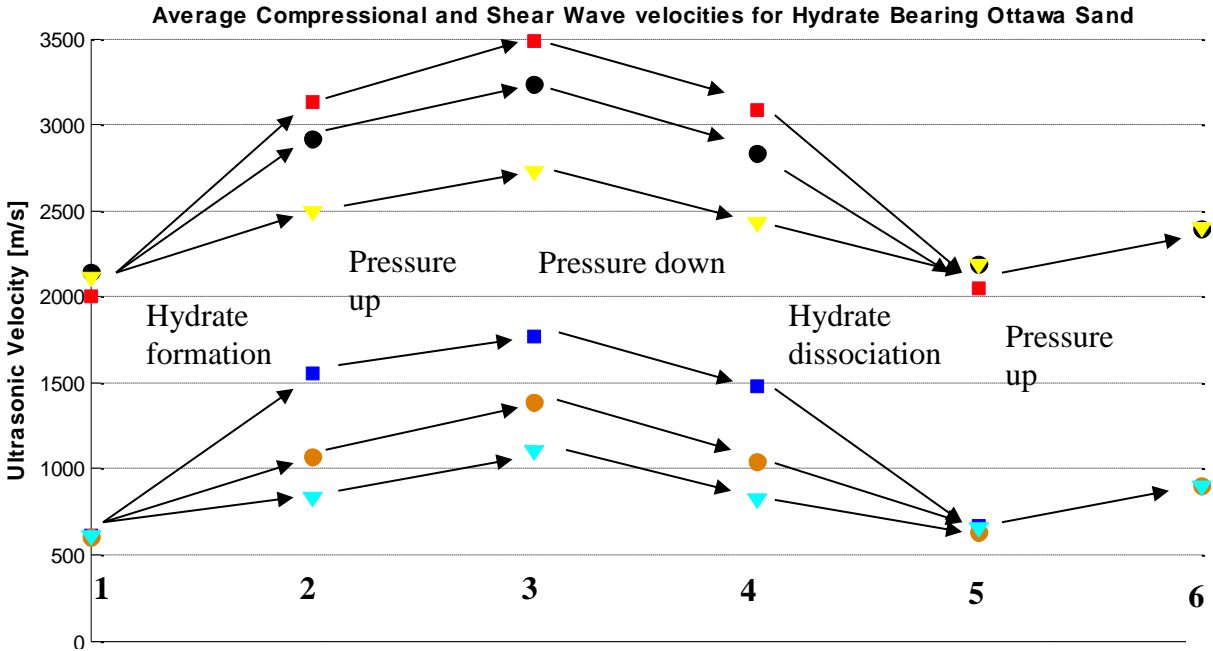


Figure 5: Average ultrasonic velocities for 80% (squares), 60% (circles), and 40% (triangles) THF hydrate bearing samples. Numbers are explained in Table 1.

Table 2: Clarification for numbers in Figure 4.

Number	Stage	Pressure (psi)	Temperature
1	Saturated, No hydrate	435	Outside Hydrate stability
2	Hydrate	435	Within Hydrate stability
3	Hydrate	2275	Within Hydrate stability
4	Hydrate	435	Within Hydrate stability
5	Saturated, No hydrate	435	Outside Hydrate stability
6	Saturated, No hydrate	2275	Outside Hydrate stability

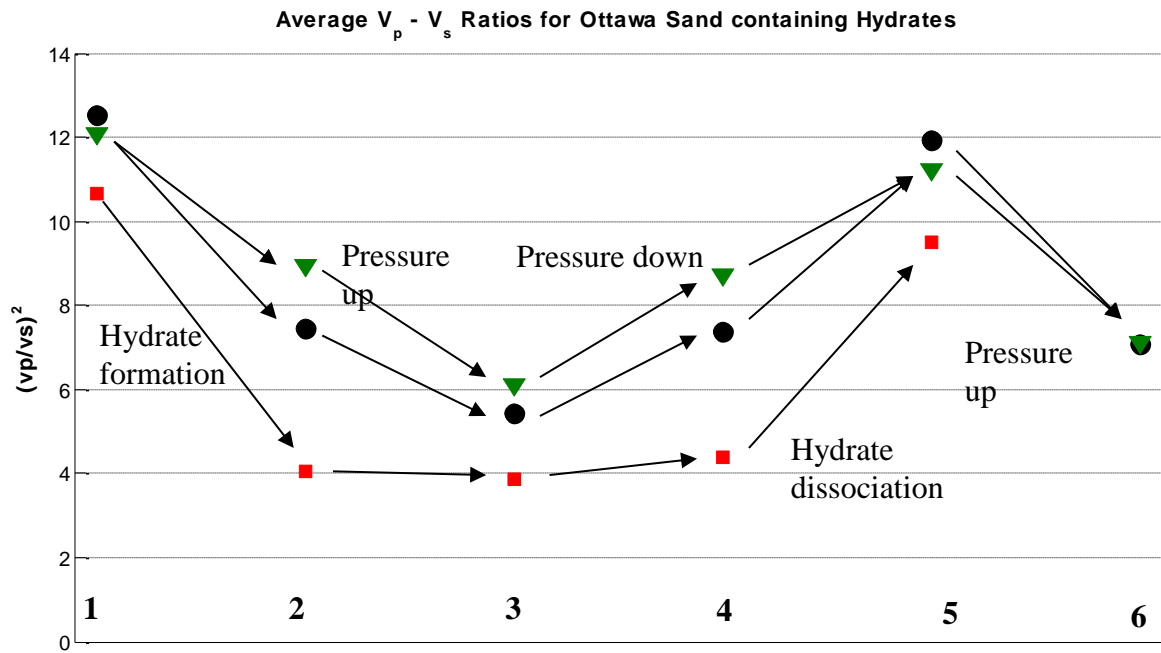


Figure 6: Average Compressional and shear wave velocity ratios for 80% (squares), 60% (circles), and 40% (triangles) THF hydrate bearing samples. Numbers are explained in Table 1

2.4 Loss Diagram (continued)

As we already have reported in Q16, we compared our initial ultrasonic velocity measurements of Ottawa sand with 80 % THF hydrate saturation with changing clay content. We saw that for samples containing 80% hydrate the data plotted in an area which corresponded to sand samples that were measured under dry conditions. We started gathering more data and plotted it in the loss diagram.

Figure 7 shows obtained data from Priest. This data is published in Priest et. al, 2006. Two different methods were used to form methane hydrates – excess gas and excess water. The excess gas method (Figure 7 – black dots) causes the hydrates to form close to the grain surfaces resulting in a noticeable increase in velocities already at low hydrate saturations. Using the excess water method (Figure 7 – green dots) the hydrate is formed in the pore space. This method requires higher amounts of hydrate to be present in the sediment to see an increase in velocities.

What we can see is that with increasing hydrate saturation, the v_p - v_s ratio decreases for the excess water method. However, this decrease does not happen until a hydrate saturation of above 30 % is present in the sample. For the excess gas method, hydrate saturations of 3 % already cause the v_p - v_s ratio to reach a value of ~5. This value only changes a little bit with increasing hydrate saturation. Two data points are not following the observed trend and show higher Q_p - Q_s ratios. But these two data points fall within an area where the well log data from Guerin and Goldberg lies.

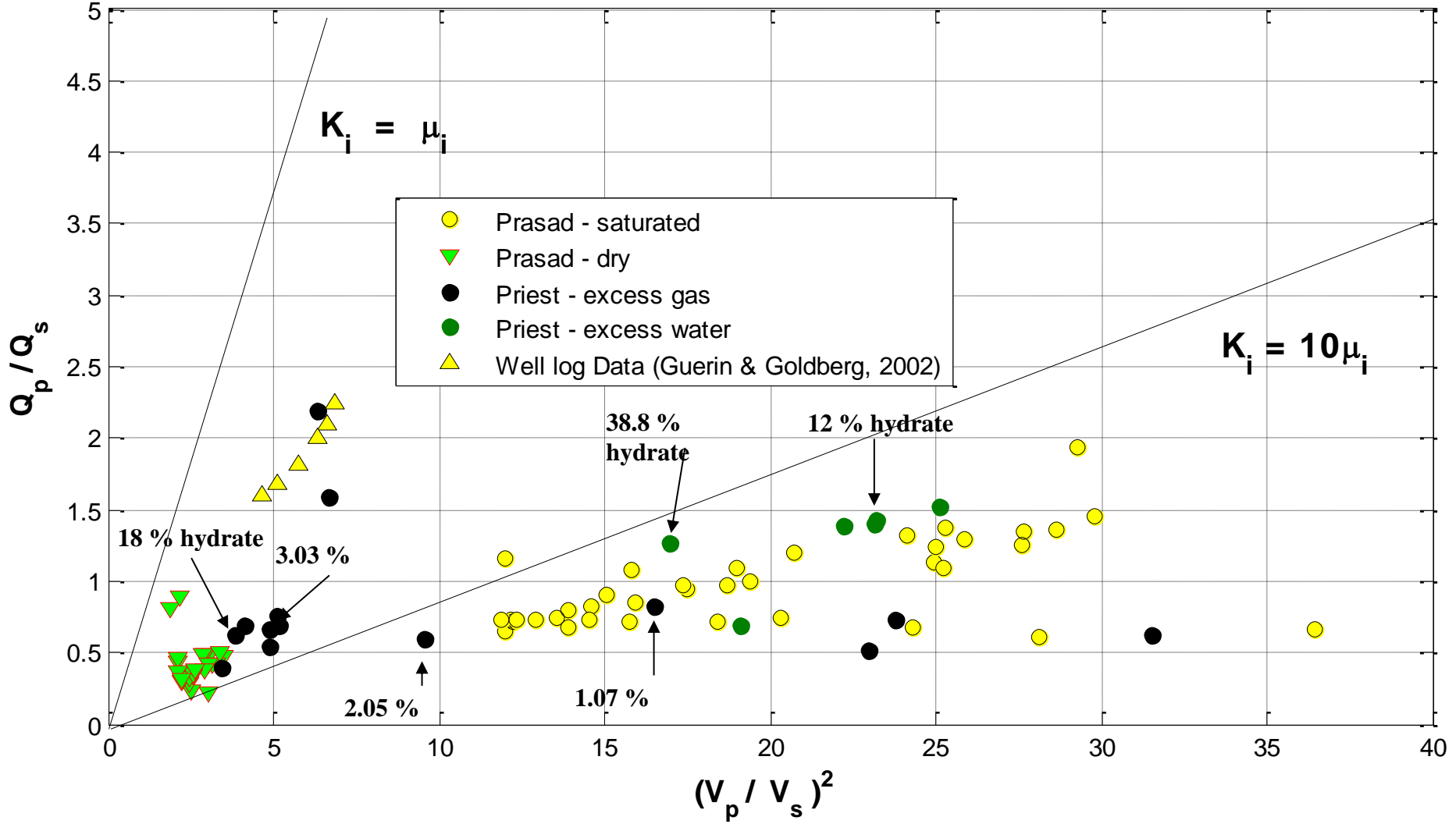


Figure 7: Loss diagram with data provided from Priest as well as well log data from Guerin & Goldberg

Using Priest's data and include our latest measurements into the loss diagram we can see that by reducing the THF hydrate saturation causes the vp-vs ratios to increase. Comparing hydrates formed with THF and methane hydrates formed with the excess water method we can see the same behavior (Figure 8). Lower hydrate saturations only change the vp-vs ratio a little bit whereas at higher hydrate saturations the vp-vs ratio decreased to a significantly lower value. Increasing the confining pressure to 2275 psi causes the vp-vs ratio for 60% and 40% to reduce even more which is in agreement with Prasad's observations that an increase in confining pressure decreases the vp-vs ratio due to compaction. We are going to calculate the Qp and Qs values for our experiments to provide absolute values instead of the bars seen in Figure 8.

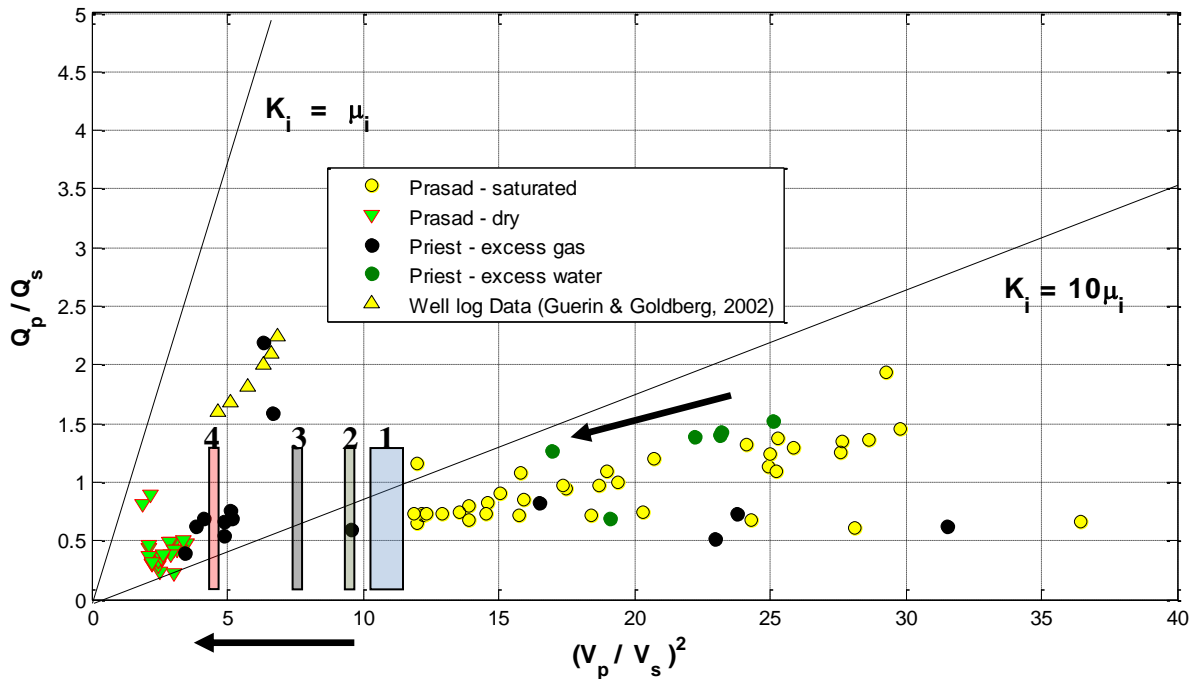


Figure 8: Loss Diagram with our obtained average vp-vs ratios for 80% (4), 60% (3), and 40% (2) THF hydrate in Ottawa sand and our samples containing THF-water mixture (1). The arrows indicate increase in hydrate saturation.

2.5 Updates to Micro X-Ray CT Pressure Control Setup

We updated our micro CT setup with a new set of ultrasonic P-wave transducers (Figure 9) which are bigger in diameter than the previous set. We further replaced the Torlon pressure cell with an aluminum cell (Figure 10) which has a bigger inner diameter and thinner walls allowing for more space inside of the cell. The cell has been pressure tested to 5000 psi (34.5 MPa). The change to a different pressure cell was necessary since the Torlon vessel did not allow enough space to insert and remove a jacketed sample with the transducers and wire clamps without causing damage to the transducers. After destroying two sets of transducers beyond repair when removing the sample from the vessel, we decided to make changes to the setup. The inner diameter of the cell is now 20.6 mm instead of 14 mm allowing us to safely insert a sample with a diameter of 12.6 mm. The transducers consist of piezoelectric PZT P-wave crystals with a diameter of 4 mm encased by cylindrical pieces of PEEK. The PZT crystal is

backed by a mixture of tungsten and epoxy to attenuate reflections from the back of the crystal. The ground wire is attached to the side of the PZT crystal facing towards the sample and is covered with a layer of conductive epoxy. The signal wire is attached to the back of the PZT crystal and held in place by the tungsten backing. To avoid leaking through the wires, we fixed them with ports at the outward facing end of the transducers and soldered wires to connect to the feed-through to the ports. The small dimensions of the transducers led us to the decision to include only P-wave crystals for now. Pore fluid lines are added to both transducers. The top transducer has a stainless steel fluid line and the bottom transducer has a flexible PEEK fluid line of 20 cm length. A hole is drilled through the entire length of the PEEK housing, the diameter of the hole is larger for the last 5 mm (1 mm diameter) to fit the fluid line. The fluid line can be connected to the feed-through pore fluid line with a Swagelok fitting. The fluid line, ports and wires are protected and sealed by a layer of flexible epoxy on the outward facing side of the transducer. No changes to the feed-through have been made. Since the aluminum cell has the same outer diameter as the Torlon cell (25.4 mm) the same feed-through as before is used.



Figure 9: Aluminum pressure cell for use inside CT scanner



Figure 10: Ultrasonic P-wave transducers for use inside micro CT scanner.

An example for a compressional waveforms collected with the transducers is shown in Figure 11. The waveforms were collected on 19.5 mm, 47.5 mm, 67.6 mm and 102.1 mm long pieces of aluminum at 22°C and atmospheric pressure. The arrival times for all 4 aluminum pieces is shown in Figure 12 together with the resulting dead time of = $t_d = 1.58 \cdot 10^{-6} \text{ s}$. P-wave velocity for aluminum was estimated as 6452 m/s. The P-wave first arrival has amplitudes of 20 to 60 mV proving that we will be able to obtain sufficient signal quality to reliably pick first arrival times. A higher signal quality than with the previous transducers has been accomplished by changing the shape of the transducer backing in order to avoid reflections from the backing.

3. Conclusion

The main findings of our project have been as follows:

Hydrate formation Process: Using complex electrical conductivity measurements, we show how to distinguish between initiation and completion of the hydrate formation process.

Free water presence: We have successfully documented that even after the hydrate formation was completed, we still had free water in the sample that converted to ice after lowering the temperature below the freezing point of water. The measurements of acoustic velocity and attenuation, electrical conductivity, and MXCT images before and after methane hydrate formation documented our finding.

Hydrate Location: Hydrate are not cementing at low concentration: (a) The increase in ultrasonic velocity after hydrate formation gets increasingly smaller with decreasing hydrate saturation; (b) At low hydrate concentration, there is a larger increase in velocities with increasing confining pressure. Cementing hydrate would create a stiffer framework and prevent large compaction-driven increases in velocity. Effects of hydrate cementation are more pronounced in Vp-Vs ratios. These measurements provide a diagnostic tool to detect hydrate saturations.

Data comparison and dissemination: We obtained velocity and attenuation data for methane hydrates formed using the excess gas and excess water method. Data from the excess gas method shows that already small amounts of hydrate have a strong influence on the vp-vs ratio (hydrate saturations of about 3%). Whereas the data from methane hydrates formed with the excess water method shows that changes start to occur at higher gas hydrate saturations (>30 %). A comparison of methane hydrate data formed using the excess water method with our THF hydrate data show a great match. In both cases, the decreases in Vp-Vs ratio with increasing hydrate saturation are comparable.

Measurement system: We built a new set of ultrasonic P-wave transducers and a new aluminum pressure cell for the use inside of the CT scanner with a bigger inner diameter than the previously used Torlon cell. The cell has been pressure tested and the ultrasonic transducers have been proven to work.

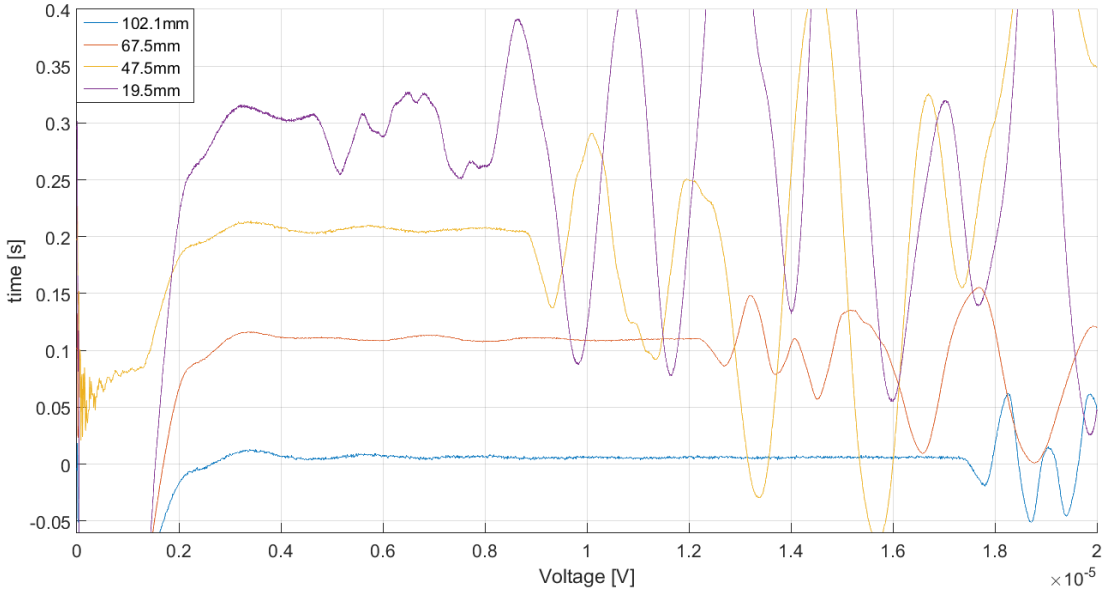


Figure 11: Waveforms for 4 pieces of aluminum – 19.5 mm, 47.6 mm, 67.5 mm and 102.1 mm long

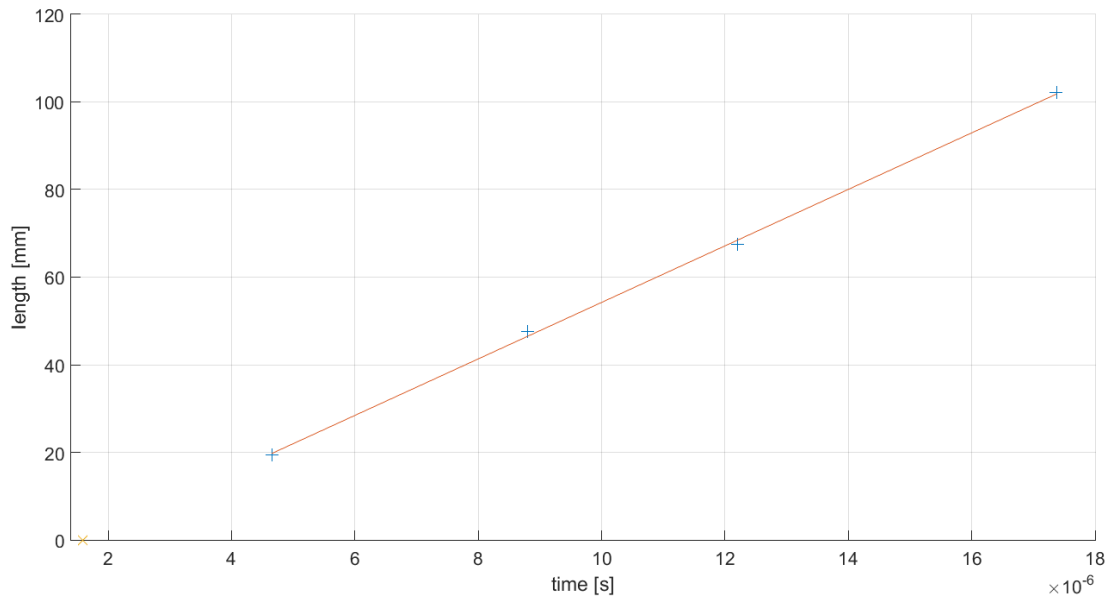


Figure 12: arrival times for all 4 aluminum pieces (blue) and dead time (yellow)

4. Acknowledgments

This project is funded by the U.S. Department of Energy (DOE) National Energy Technology Laboratory (NETL) under Grant Number DEFE0009963. This project is managed and administered by the Colorado School of Mines and funded by DOE/NETL and cost-sharing partners.

We thank the US Department of Energy for sponsoring the project. We also thank Tim Collett for his cooperation with us on this project. We acknowledge support of some personnel by other grants (DHI/Fluids and OCLASSH consortia, Chinese Mining University).

References

Revil, A, N. Florsch and C. Camerlynck (2014): "Spectral Induced Polarization Porosimetry", *Geophysical Journal International*, GJI Marine geosciences and applied geophysics, Vol. 198, p. 1016-1033

5. Plans

Table 4 shows the Milestones and Deliverables for this quarter. We plan to focus on CH₄ hydrates in MXCT scanning. We are delayed in Milestone 7. Due to various delays in our experimentation and initial attempts failing to form methane out of the free gas phase, we anticipate a more realistic completion date of 12/31/2016. We needed to improve our experimental setup for P- and S-wave measurements due to leaks and poor signal quality. We plan to continue these measurements for the remaining samples. In addition to methane hydrate experiments, we will also perform methane – CO₂ exchange experiments to study their effects on acoustic, elastic, and attenuation properties.

We plan to extend our comparison of our attenuation results for sand packs with and without clay with more field data as well as with laboratory for methane hydrate bearing and ice bearing sand samples.

We are planning on performing MXCT measurements with our newly designed and tested feed-throughs to visually and acoustically observe methane hydrate formation in sediment out of the free gas phase. Further, we plan to compare our measured ultrasonic velocities with effective medium models and numerical finite difference models based on the micro CT images.

Table 3: Q17 Milestones and Deliverables

Milestone	Task	Description	Completion date	Report Content
7	6	Methane hydrates from free gas phase (incomplete)	12/31/2016	Progress report
10	9	NMR/MXCT characterization	12/31/2016	Progress report
13	12	Information Dissemination	12/31/2016	Progress report

5. Products

Publications (Publications; Conference Papers, Presentations, Books)

Nothing to report

Website or other Internet sites

<http://crusher.mines.edu/CRA-DOE-Hydrates>

Technologies or techniques

Nothing to report

Inventions, patent applications and/or licenses

Nothing to report

Other Products

Nothing to report

6. Participants and Collaborating Organizations

CSM personnel:

Name:	Manika Prasad
Project Role:	Principle Investigator
Nearest person month worked this period:	0.25
Contribution to Project:	Dr. Prasad helped with acoustic and attenuation measurements.
Additional Funding Support:	Academic faculty
Collaborated with individual in foreign country:	No
Country(ies) of foreign collaborator:	N/A
Travelled to foreign country:	Yes
If traveled to foreign country(ies),	India, Norway
Duration of stay:	1 months

Name:	Michael Batzle †
Project Role:	Principle Investigator
Nearest person month worked this period:	0
Contribution to Project:	Dr. Batzle was responsible for the overall (dis)organization of the project.
Additional Funding Support:	Academic faculty
Collaborated with individual in foreign country:	No
Country(ies) of foreign collaborator:	N/A
Travelled to foreign country:	No
If traveled to foreign country(ies),	N/A
Duration of stay:	N/A

Name:	Carolyn Koh
Project Role:	Co-Investigator
Nearest person month worked this period:	0.25
Contribution to Project:	Dr. Koh helped with CH ₄ hydrate experimental setup and measurements
Additional Funding Support:	Academic faculty
Collaborated with individual in foreign country:	No
Country(ies) of foreign collaborator:	N/A
Travelled to foreign country:	No
If traveled to foreign country(ies),	N/A
Duration of stay:	N/A

Name:	Weiping Wang
Project Role:	Laboratory Manager

Nearest person month worked this period:	1
Contribution to Project:	Mr. Wang assisted in equipment fabrication
Additional Funding Support:	DHI/Fluids consortium, Chinese Mining University
Collaborated with individual in foreign country:	No
Country(ies) of foreign collaborator:	N/A
Travelled to foreign country:	No
If traveled to foreign country(ies):	N/A
duration of stay: N/A:	N/A

Name:	Mathias Pohl
Project Role:	Ph.D. student
Nearest person month worked this period:	1
Contribution to Project:	Mr. Pohl prepared samples and pressure tested new equipment.
Additional Funding Support:	N/A
Collaborated with individual in foreign country:	No
Country(ies) of foreign collaborator:	N/A
Travelled to foreign country:	Yes
If traveled to foreign country(ies)	Germany
duration of stay:	N/A

Name:	Mandy Schindler
Project Role:	Ph.D. student
Nearest person month worked this period:	3
Contribution to Project:	Ms. Schindler prepared samples and collected CT data.
Additional Funding Support:	N/A
Collaborated with individual in foreign country:	No
Country(ies) of foreign collaborator:	yes
Travelled to foreign country:	Germany
If traveled to foreign country(ies),	N/A
duration of stay:	3 weeks

Name:	Ahmad Afif Abdul Majid
Project Role:	Post Doctoral Scholar
Nearest person month worked:	1
Contribution to Project:	Dr. Majid helped setting up our experiment to form methane hydrates out of free gas
Additional Funding Support:	Center for Hydrate Research
Collaborated with individual in foreign country:	No
Country(ies) of foreign collaborator:	N/A
Travelled to foreign country:	No

If traveled to foreign country(ies):	N/A
duration of stay:	N/A

External Collaborations:

Dr. Tim Collett
US Geologic Survey
Denver, Colorado

Support: Dr. T. Collett provided data and guidance on interpretation and application. He continues to publish numerous papers on hydrate properties.

7. Changes / Problems

We requested and were granted a no-cost extension until December 31, 2016. The extension was necessitated due to delays and disruptions in our scheduled work caused by a change in PI and the need to rebuild equipment. The older equipment was not suitable for methane hydrate work. We have built a new system and have completed pressure tests on the newly built system. Thus, we anticipate making our measurements on methane hydrates in the coming months.

Mathias Pohl was interning for the months of May and June and thus had to interrupt his experimental work. Cesar Mapeli and Mandy Schindler continued his work on methane-hydrate bearing sediments.

8. Special Reporting Requirements

None

9. Budgetary Information

Attached separately